

Disulfide-Linked, Gold Nanoparticle Based Reagent for Detecting Small Molecular Weight Thiols

Suzanne Durocher,[†] Asad Rezaee,[‡] Caroline Hamm,[†] Chitra Rangan,[§] Silvia Mittler,[‡] and Bulent Mutus*,[†]

Departments of Chemistry & Biochemistry and Physics, University of Windsor, 401 Sunset Avenue, Windsor, Ontario, Canada, and Department of Physics and Astronomy, The University of Western Ontario, London, Ontario, Canada

Received October 30, 2008; E-mail: mutusb@uwindsor.ca

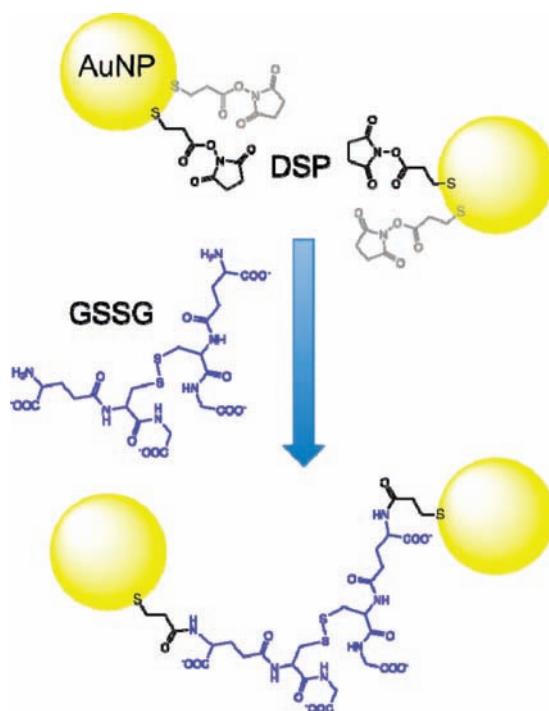
The reduced to oxidized (redox) ratio of thiols on proteins freely circulating in blood or attached to the surfaces of vascular cells is under strict regulation since small alterations in the redox status of proteins in the circulatory system can adversely affect diverse physiological phenomena including blood coagulation, glucose uptake/release, NO_x-mediated vascular contraction/relaxation, gene expression, and immunological and hormonal responses.^{1–15} The redox status of blood is maintained by circulating low molecular weight (<350 Da) thiols (LMWTs) such as hydrogen sulfide,^{16,17} cysteine (Cys), homocysteine (HCys), glutathione (GSH), γ -glutamyl-cysteine (γ -Glu-Cys), and cysteinylglycine (Cys-Gly). There are many reagents for the spectroscopic determination (by UV/vis or fluorescence) of the levels of total (high molecular weight thiols (HMWTs) + LMWTs) in biological fluids.^{2,18–22} The coupling of these reagents with specialized instrumental techniques including HPLC, CE, and LC–MS² allows for the identification and quantification of LMWTs as well as HMWTs. However, there are no stand-alone spectroscopic methods for reagents that specifically detect LMWTs but not HMWTs.

The aim of the present study was to develop a colorimetric reagent that specifically reacted with LMWT but not with HMWT. Our strategy was to place a disulfide bridge in a steric environment that was accessible to reduction by LMWT but not by HMWT. In addition, the disulfide cleavage would have to be accompanied by a spectral change that could signal the presence of LMWTs. Gold nanoparticles appeared to be ideal candidates from both the steric and the reporter points of view: theoretically, disulfide-linked AuNP clusters would act to limit the size of molecules that can access the disulfide bond provided the length of the spacer linking the disulfides is short; and monodisperse AuNPs have different LSPR spectral properties than AuNP clusters^{23,24} thus providing a signal for disulfide cleavage.

We synthesized ~10–12 nm citrate-capped AuNP by a previously published method where HAuCl₄ (1 mM) was boiled under reflux and mixed with sodium citrate (38.8 mM).²⁵ The resultant red liquid was filtered through a 0.8 μ m Gelman filter and utilized as the AuNP stock solution throughout the studies.

The synthesis of disulfide-cross-linked AuNP clusters was accomplished by first coating the gold surface of the AuNP with dithiobis[succinimidyl]propionate (DSP). This would have two beneficial effects: (1) saturation of the AuNP surface with thiols ensures that this complex would be inert to reactions with the disulfide-linked cross-linker used to form the AuNP clusters; and (2) the amine-reactive succinimidyl residue would be exposed to solvent ideal for a reaction with the amine groups of the glutathione

Scheme 1. Synthesis of Disulfide-Linked AuNP Clusters



disulfide (GSSG) which was employed as the disulfide-containing cross-linker (Scheme 1).

In order for this strategy to be successful we had to ensure that the AuNPs were saturated with DSP. To monitor DSP saturation we took advantage of the observation that the rate of hydrolysis of the succinimidyl group (increase in absorbance with a λ_{max} 260nm)²⁶ was greatly reduced in the presence of AuNPs (Figure 1). This is clearly observed in Figure 1: when increasing amounts of DSP are added to buffer alone, the initial rates of hydrolysis increase linearly with increasing [DSP] (Figure 1, green diamonds). However, in the presence of AuNP (Figure 1, pink diamonds) the slope of the increase in the initial rates between 0.5 nmol to 1.25 nmol DSP was ~9-fold lower than that observed in buffer alone. At [DSP] > 1.25 nM the initial rates increased with a similar slope to that observed in buffer, an indication of the DSP saturation point for a given amount of AuNP. This phenomenon is likely related to the limited solvent accessibility of the propionate carbonyl to attack by H₂O in the case of the AuNP-bound DSP.

The sequence of reagent additions was crucial to obtaining disulfide-linked AuNPs. A saturating amount of DSP (3 μ M; calculated from a titration as in Figure 1) was added first to the AuNPs (50 μ L in 450 μ L phosphate buffer, 10 mM, pH 9.4) and

[†] Department of Chemistry & Biochemistry, University of Windsor.

[‡] The University of Western Ontario.

[§] Department of Physics, University of Windsor.

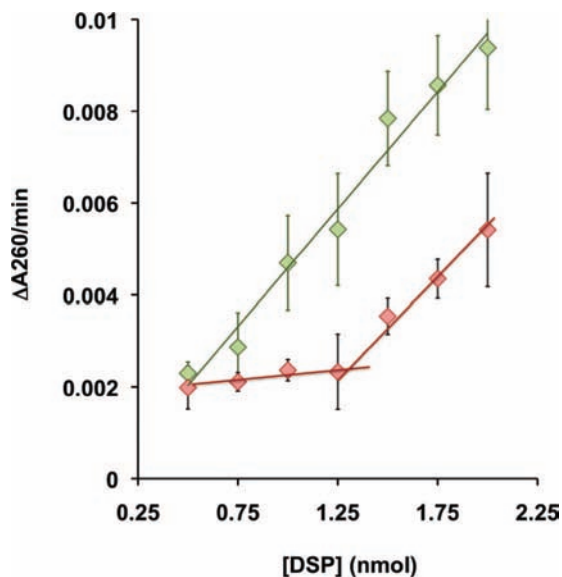


Figure 1. Initial rates of DSP hydrolysis (monitored at 260 nm) for increasing amounts of DSP in 10 mM phosphate buffer pH 9.4 (green diamonds) or in 10 mM phosphate buffer pH 9.4 containing 50 μL of AuNP (pink diamonds). In each case, the total volume was 500 μL .

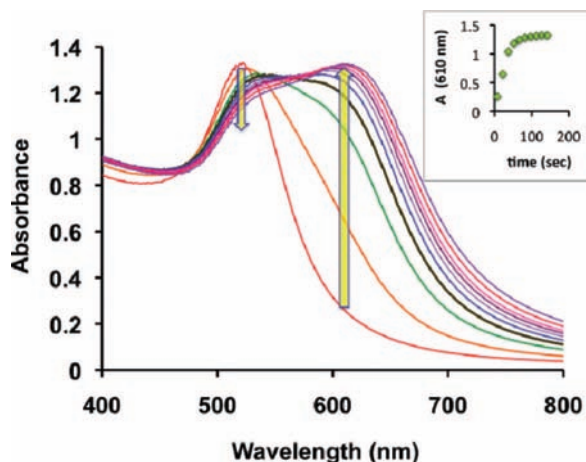


Figure 2. Spectral changes of the LSPR accompanying disulfide-linked AuNP cluster formation. AuNP plus DSP after 60 s of incubation, leftmost scan (red line) with $\lambda_{\text{max}} = 520$ nm; scans at 15 s intervals after GSSG addition. Inset: plot of increase at 610 nm at 15 s intervals, subsequent to GSSG addition.

incubated for ~ 1 min followed by the addition of GSSG (7.0 mM) to the mixture (final volume = 500 μL). The monodispersed AuNP plasmon band ($\lambda_{\text{max}} = 520$ nm) broadened and red-shifted ($\lambda_{\text{max}} = 610$ nm) as the AuNP clusters formed (Figure 2). Under the conditions employed, the cross-linking reaction was complete within 75 s (Figure 2, inset).

AuNP cluster formation was confirmed by transmission electron microscopy (Figure 3). The AuNP clusters were stable once formed since the ratio of the absorbance 520 to 610 nm remained constant for 24 h (at room temperature in a 1.5 mL polypropylene centrifuge tube).

The AuNP clusters were exposed to identical concentrations (1 μM) of thiols varying in molecular weight (38 Da to 66 000 Da). In the presence of the thiols the deep blue color of the solution, due to AuNP clusters absorbing in the red, changed to red, absorbing in the blue, characteristic of monodisperse AuNP (Figure 4 A) LSPR. Spectroscopic analysis of the thiol-induced color change

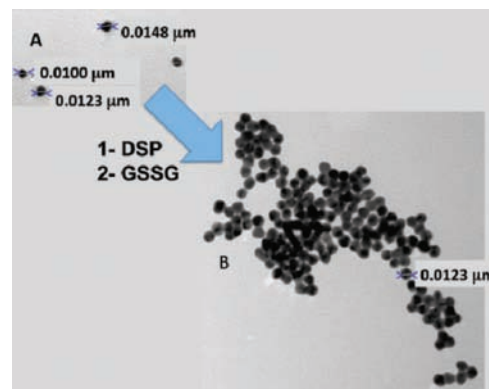


Figure 3. Transmission electron micrographs of monodisperse AuNP (A) and disulfide-linked AuNP clusters (B).

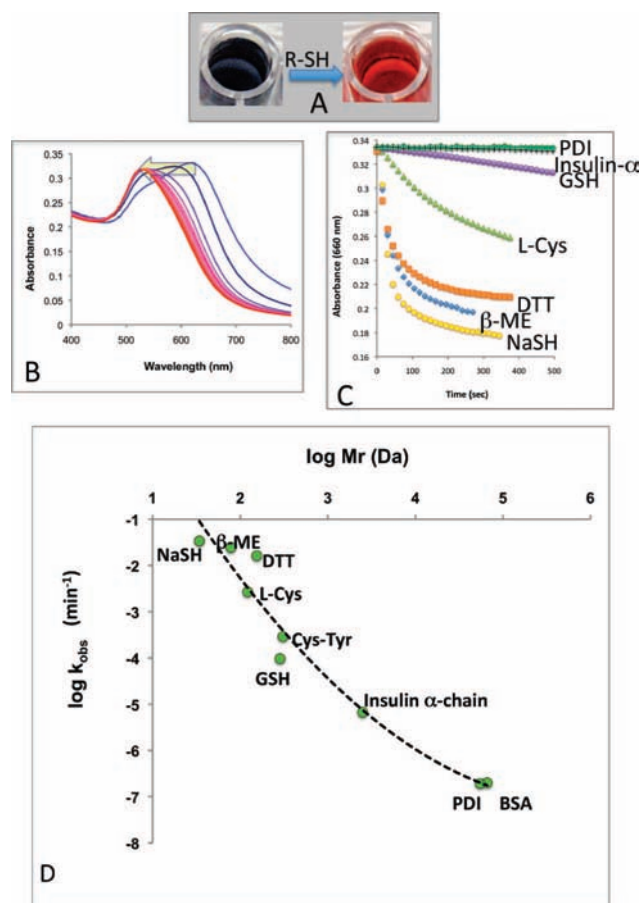


Figure 4. Effect of thiols on disulfide-linked AuNP clusters. Color (A) and spectral (B) LSPR response accompanied by introduction of thiols (here: dithiothreitol, 1 μM) to SSAuNPs. The kinetic change at $\lambda = 610$ nm of SSAuNPs reduction by thiols (1 μM) of varying molecular weight (C). A log/log plot of the pseudo-first-order rate constants of disulfide-linked to monodisperse AuNP formation as a function of molecular weight of the thiols: Sodium hydrosulfide, NaSH; β -mercaptoethanol, β -ME; dithiothreitol, DTT; L-Cysteine, Cys; cysteinyltyrosine, Cys-Tyr; glutathione, GSH; insulin α -chain; protein disulfide isomerase, PDI; bovine serum albumin, BSA (D).

indicated that this process was essentially the reverse of the formation of AuNP clusters (Figure 4B, Figure 2). The temporal analysis of the thiol reduction yielded an inverse proportionality to the thiol size, and above a molecular weight of ~ 310 Da, the AuNP cluster to monodisperse transition was essentially undetectable (Figure 4C). This is revealed in a plot of the pseudo-first-

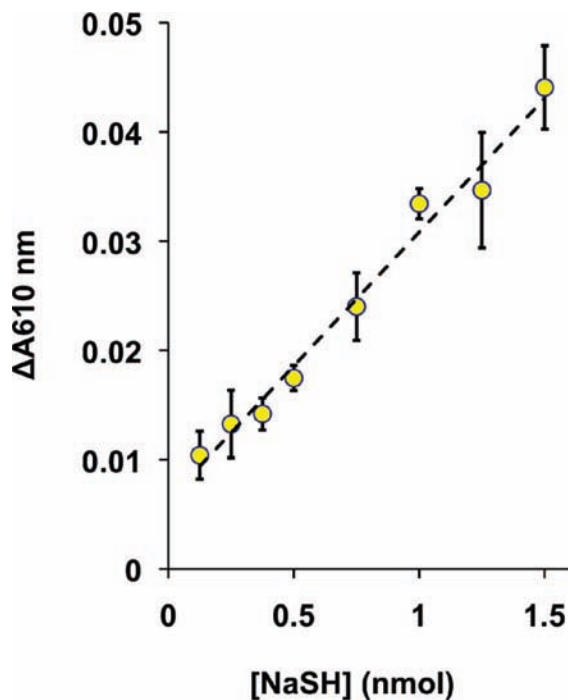


Figure 5. Increasing amounts of NaSH were added to SSAuNPc (with a total capacity of reacting with 15.7 μM thiol) in phosphate buffer, 10 mM, pH 7.4. The initial absorbance of this solution at 610 nm was 0.2. The reaction volume was 500 μL . The error bars represent standard deviation ($n = 3$). The equation of the best-fit line was $y = 0.0245x + 0.0063$ ($R^2 = 0.983$).

order rate constants (k_{obs} ; calculated from a plot of $\ln(\Delta A_{610 \text{ nm}})$ vs t) of disulfide-linked to monodisperse AuNP formation as a function of molecular weight of the thiols employed (Figure 3 D); NaSH cleaved the disulfides with rate constants that were ~ 120 -fold and 5000-fold larger than those for glutathione and insulin α -chain, respectively. In the case of the protein thiols (BSA and PDI) the disulfide cleavage rates were 170 000-fold slower than that observed with NaSH.

We also estimated a pseudoextinction coefficient for the disulfide-linked AuNP clusters (SSAuNPc) of 12 700 $\text{M}^{-1} \text{cm}^{-1}$ by determining the amount of NaSH required to totally eliminate the AuNP cluster-dependent absorbance at 610 nm (Figures 3 and 4B). In addition, the thiol detection limit of the SSAuNPc was determined to be ~ 0.125 nmol from a plot of the decrease at 610 nm vs [NaSH] (Figure 5). The estimated extinction coefficients and detection limits for SSAuNPc are very similar to those of a commonly employed thiol reagent 5,5'-dithiobis-2-nitrobenzoate which has an extinction coefficient of 13 600 $\text{M}^{-1} \text{cm}^{-1}$ at 412 nm.²⁷ This means that SSAuNPc can be used to detect physiologically important LMWT like H_2S whose plasma concentrations range between ~ 10 and 40 μM .^{16,17,28}

In this study, we were successful in synthesizing disulfide-linked AuNP clusters (SSAuNPc) and showed that the particularly chosen disulfide bond was accessible to reduction by thiols up to a

molecular weight above ~ 310 Da. These properties make SSAuNPc the first reagent that can selectively detect LMWT thiols. We expect to be able to control the molecular weight at which the AuNP cluster to monodisperse transition occurs, by systematically varying the spacer length between the disulfide moiety and the AuNP. Potential applications of SSAuNPc include the determination of the levels of LMWT pools in biological fluids; detection of LMWT reducing agent contamination in industrial scale protein purification; and as sensors for volatile, toxic LMWT thiols like H_2S .

Acknowledgment. This study was supported by an operating grant from the Windsor Regional Cancer Centre Local Investigators Research Fund (WRCC-LIRF) and an NSERC Discovery Grant (to B.M.). Research contributions of S.M. were supported by the Canada Research Chair (Tier 1) program, OAML, and an OCE AuTEK grant. C.R. gratefully acknowledges support from NSERC.

References

- (1) Wood, P. L.; Khan, M. A.; Moskal, J. R. *Brain Res.* **2007**, *1158*, 158–63.
- (2) Rafii, M.; Elango, R.; Courtney-Martin, G.; House, J. D.; Fisher, L.; Pencharz, P. B. *Anal. Biochem.* **2007**, *371* (1), 71–81.
- (3) Oktyabrsky, O. N.; Smirnova, G. V. *Biochemistry (Mosc)* **2007**, *72* (2), 132–45.
- (4) Liang, M.; Pietrusz, J. L. *Arterioscler. Thromb. Vasc. Biol.* **2007**, *27* (1), 77–83.
- (5) Franco, R.; Schoneveld, O. J.; Pappa, A.; Panayiotidis, M. I. *Arch. Physiol. Biochem.* **2007**, *113* (4–5), 234–58.
- (6) Pop, S. M.; Gupta, N.; Raza, A. S.; Ragsdale, S. W. *J. Biol. Chem.* **2006**, *281* (36), 26382–90.
- (7) Pantano, C.; Reynaert, N. L.; van der Vliet, A.; Janssen-Heininger, Y. M. *Antioxid. Redox Signal* **2006**, *8* (9–10), 1791–806.
- (8) Na, H. K.; Surh, Y. J. *Mol. Carcinog.* **2006**, *45* (6), 368–80.
- (9) Fiaschi, T.; Cozzi, G.; Raugei, G.; Formigli, L.; Ramponi, G.; Chiarugi, P. *J. Biol. Chem.* **2006**, *281* (32), 22983–91.
- (10) Biswas, S.; Chida, A. S.; Rahman, I. *Biochem. Pharmacol.* **2006**, *71* (5), 551–64.
- (11) Wu, G.; Fang, Y. Z.; Yang, S.; Lupton, J. R.; Turner, N. D. *J. Nutr.* **2004**, *134* (3), 489–92.
- (12) Liu, J. D.; Tsai, S. H.; Lin, S. Y.; Ho, Y. S.; Hung, L. F.; Pan, S.; Ho, F. M.; Lin, C. M.; Liang, Y. C. *Life Sci.* **2004**, *74* (19), 2451–63.
- (13) Kondo, N.; Ishii, Y.; Son, A.; Sakakura-Nishiyama, J.; Kwon, Y. W.; Tanito, M.; Nishimaka, Y.; Matsuo, Y.; Nakayama, T.; Taniguchi, M.; Yodoi, J. *Immunol. Lett.* **2004**, *92* (1–2), 143–7.
- (14) Barford, D. *Curr. Opin. Struct. Biol.* **2004**, *14* (6), 679–86.
- (15) Hildebrandt, W.; Droge, W. *Forum Nutr.* **2003**, *56*, 199–200.
- (16) Kimura, H.; Nagai, Y.; Umemura, K.; Kimura, Y. *Antioxid. Redox Signal* **2005**, *7* (5–6), 795–803.
- (17) Whitfield, N. L.; Kreimler, E. L.; Verdial, F. C.; Skovgaard, N.; Olson, K. R. *Am. J. Physiol. Regul. Integr. Comp. Physiol.* **2008**, *294* (6), R1930–7.
- (18) Carru, C.; Deiana, L.; Sotgia, S.; Pes, G. M.; Zinellu, A. *Electrophoresis* **2004**, *25* (6), 882–9.
- (19) Ivanov, A. R.; Nazimov, I. V.; Baratova, L. *J. Chromatogr. A* **2000**, *895* (1–2), 157–66.
- (20) Causse, E.; Terrier, R.; Champagne, S.; Nertz, M.; Valdiguie, P.; Salvayre, R.; Couderc, F. *J. Chromatogr. A* **1998**, *817* (1–2), 181–5.
- (21) Kang, S. H.; Kim, J. W.; Chung, D. S. *J. Pharm. Biomed. Anal.* **1997**, *15* (9–10), 1435–41.
- (22) Hogan, B. L.; Yeung, E. S. *Anal. Chem.* **1992**, *64* (22), 2841–5.
- (23) Jensen, T.; Kely, L.; Lazarides, A.; Schatz, G. C. *J. Cluster Sci.* **1999**, *10*, 295–317.
- (24) Mirkin, C. A.; Letsinger, R. L.; Mucic, R. C.; Storhoff, J. J. *Nature* **1996**, *382* (6592), 607–9.
- (25) Grabar, K. C.; Freeman, R. G.; Hommer, M. B.; Natan, M. J. *Anal. Chem.* **1995**, *67*, 735–743.
- (26) Carlsson, J.; Drevin, H.; Axen, R. *Biochem. J.* **1978**, *173*, 723–37.
- (27) Silverstein, R. M. *Anal. Biochem.* **1975**, *63* (1), 281–2.
- (28) Zhu, Y. Z.; Wang, Z. J.; Ho, P.; Loke, Y. Y.; Zhu, Y. C.; Huang, S. H.; Tan, C. S.; Whiteman, M.; Lu, J.; Moore, P. K. *J. Appl. Physiol.* **2007**, *102* (1), 261–8.

JA808548X